# 3-D Fast Imaging Method for UWB Radar in Interference-Rich Environments with Global Optimization

Takuya Sakamoto†, Hiroshi Matsumoto‡, and Toru Sato††

Graduate School of Informatics, Kyoto University
Yoshida-Honmachi, Sakyo-ku, Kyoto, 606-8501, Japan

E-mail: †t-sakamo@i.kyoto-u.ac.jp, ‡h-matumo@aso.cce.i.kyoto-u.ac.jp, ††tsato@kuee.kyoto-u.ac.jp

**Abstract** The SEABED method, a fast imaging algorithm for UWB pulse radar systems, makes it possible to image 3-D unknown targets using a reversible transform between the target shape and antenna position. The antenna position and distance form a curved surface called a "quasi-wavefront". We can estimate the target shape directly using this transform if we can extract the quasi-wavefront from the observed data. In the case of complex-shaped targets, however, it is difficult to obtain the correct image because the received signals interfere with each other through the echoes from multiple reflected points. Conventional methods, that extract the quasi-wavefront at each antenna position, suffer from a serious fault in that the values obtained in the region with interference are not accurate. To overcome this problem, we propose a simultaneous estimation of all quasi-wavefronts from the received signal waveforms at all antenna positions by treating the problem as an optimization of an evaluation function.

**Key words** UWB, radar, interference, SEABED, imaging

## 1. Introduction

The fast imaging algorithm for UWB pulse radar systems, SEABED [1] is regarded as a promising near-field measuring method for real-time applications such as robotics and surveillance systems. This algorithm makes use of a reversible transform between the target shape and propagation delay. Equi-phase surfaces of the signals received at multiple positions are called quasi-wavefronts. If these quasi-wavefronts are correctly estimated, fast and accurate imaging can be achieved using SEABED, which is faster than other methods such as the synthetic aperture method [2], [3]. For complex-shaped targets, however, it is difficult to extract quasi-wavefronts because echoes from multiple scattering centers interfere with one another. This problem means that while SEABED works well for a single simple-shaped target [1], [4], it cannot be used to estimate the shape of targets in general. Another imaging technique, the fuzzy-SEABED method, has been proposed to overcome the interference problem [6]. This method is stable even in interference-rich environments because it is based on a fuzzy function for the DOA (Direction-Of-Arrival) estimation. Good results are achieved in some cases, the approach does not completely solve the interference problem.

This paper proposes a revised version of the SEABED algorithm, using an optimization approach for extracting quasi-wavefronts. The objective function for the optimization uses the waveform information, which is not used in either the conventional SEABED or fuzzy-SEABED imaging method. Various numerical simulations show quantitatively that our proposed method can obtain accurate images even when two targets are close together.

## 2. Imaging Algorithm for UWB Radar Systems

### 2.1 System Model

Figure 1 shows the assumed system model, in which an omni-directional antenna is used for transmitting and receiving UWB pulses, and is scanned on the $x$-$y$ plane. The antenna position is defined by $(X, Y, 0)$. Targets are set in the upper area $z > 0$ and have clear boundaries. The propagation speed $c$ is assumed to be constant and known.

A strong echo is received if the antenna is positioned on the normal direction of a target surface. The distance between the antenna and this scattering center is measured repetitively. The antenna is scanned in the area $X_{\min} \leq X \leq X_{\max}$, $Y_{\min} \leq Y \leq Y_{\max}$ and the data obtained at discrete points with a constant interval of $\Delta d_x$, $\Delta d_y$. The position for data $(X_i, Y_j)$ is expressed as

$$\begin{pmatrix} X_i \\ Y_j \end{pmatrix} = \begin{pmatrix} X_{\min} + i\Delta d_x \\ Y_{\min} + j\Delta d_y \end{pmatrix} (i, j = 1, 2, \cdots, A). \quad (1)$$

The transmitting waveform $p_0(t)$ is a mono-cycle pulse with the center frequency $f = 1/\lambda$ and the pulse-width equal to the center wavelength. The normalized distance between the antenna and a scattering center $Z$ is measured as $Z = ct/2$, where $c$ is the propagation velocity and $t$ the time delay. The output of a matched filter applied to the received signal at antenna position $(X, Y, 0)$ is expressed as $s(X, Y, Z)$. In addition, we assume that the reference waveform $p(Z)$ is known and calculated as the auto-correlation

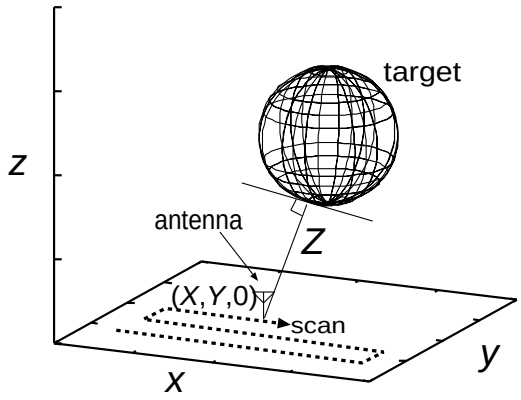


Fig. 1. System model.

function of the transmitted waveform $p_0(t)$, which is equivalent to the output of the matched filter.

### 2.2 Principle of the SEABED method

Sakamoto and Sato[1] showed the existence of the reversible transforms, BST (Boundary Scattering Transform) and IBST (Inverse BST), between a point on the target surface $(x, y, z)$ and the quasi-wavefront $(X, Y, Z)$. The SEABED algorithm first extracts the quasi-wavefronts $(X, Y, Z)$ from the received signals $s(X, Y, Z)$, and then applies the IBST to these quasi-wavefronts. The IBST is expressed as

$$\begin{cases} x &= X - Z\partial Z/\partial X, \\ y &= Y - Z\partial Z/\partial Y, \\ z &= Z\sqrt{1-(\partial Z/\partial X)^2-(\partial Z/\partial Y)^2}. \end{cases} \quad (2)$$

It is easy to extract quasi-wavefronts for a simple target shape, making it possible to obtain an accurate image within a short time [1]. For targets with complex shapes or multiple targets set close together, however, the received signal consists of multiple overlapped echoes. This makes the extraction of quasi-wavefronts difficult and unsuitable for conventional fast methods that does not work adequately.

### 2.3 Conventional Method for Extracting Quasi-Wavefronts

The original SEABED [1] extracts peaks of $s(X, Y, Z)$ and sequentially connects these peak points. If multiple candidate points exist, we select the nearest one for connection. This method, called the "peak connection method" , is simple and fast, but cannot be used for signals with interference.

Hantscher *et al.*[4] proposed the following method. First, the maximum absolute value of the received signal $s(X, Y, Z) = s_1(X, Y, Z)$ is detected as

$$Z_1 = \max_Z |s_1(X, Y, Z)|, \quad (3)$$

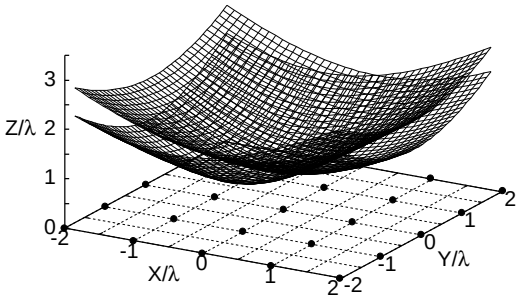


Fig. 2. True quasi-wavefronts.

where we introduce the index $s_1$ to simplify the explanation of the iteration procedure in the method. Next, the reference waveform $p(Z)$ is subtracted from the original signal

$$s_2(X, Y, Z) = s_1(X, Y, Z) - p(Z - Z_1). \quad (4)$$

Similarly, $Z_2$ is extracted from $s_2(X, Y, Z)$, and this procedure is iterated. The time delays $Z_1, Z_2, \cdots$ are used as points on the quasi-wavefronts. Although this method does not work for general problems with interference, it does work to some extent for multiple echoes with large power differences. We call this method the "sequential subtraction method".

Kidera *et al.* [6] proposed an extended SEABED method that does not require quasi-wavefronts. A fuzzy-based DOA estimator was used instead of the IBST. In this method, the peak points of signals $(X, Y, Z)$ are first extracted as in the original SEABED. Here, the distance $Z$ is known, so all we need is the angle of the scattering center. A membership function is introduced and fuzzy-based estimation that is robust against interference echoes is applied to obtain the angle. We call this method the "fuzzy-SEABED method".

## 3. Numerical Examples of Conventional Imaging Methods

### 3.1 Numerical Model Used to Evaluate the Performance of Conventional Methods

In this section, the imaging performance of conventional methods is investigated using a simplified target model. We assume two metallic spherical targets in the air, that is,

1. a sphere with a $0.4\lambda$ radius and center at $(0.3\lambda, 0, 1.4\lambda)$, and
2. a sphere with a $0.2\lambda$ radius and center at $(-0.5\lambda, 0, 0.7\lambda)$

with $\lambda = 100\mathrm{mm}$ corresponding to the center frequency 3GHz. The number of points at which data is obtained is $A \times A = 39 \times 39 = 1,521$, $X_{\min} = Y_{\min} = -2\lambda$, $X_{\max} = Y_{\max} = 2\lambda$, and $\Delta d_x = \Delta d_y = 0.1\lambda$. Figure2 shows the true quasi-wavefronts under these assumptions. The quasi-wavefront for each spherical target is a hyperboloid of revolution, with the two hyperboloids intersecting each other. With regard to the propagation model, Born approximation is assumed, and free space losses are

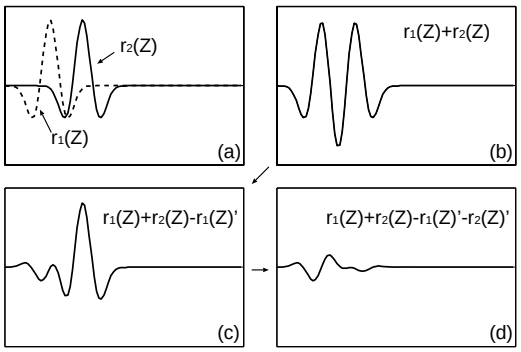


Fig. 3. Interference reduction process using the sequential subtraction method.

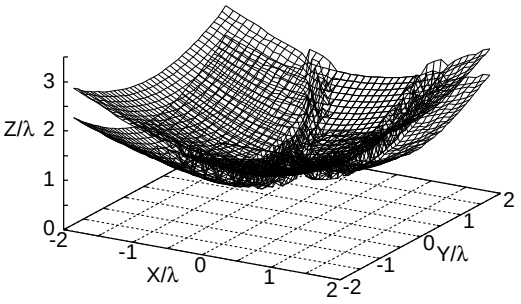


Fig. 4. Estimated quasi-wavefronts using the sequential subtraction method.

ignored for simplicity. For antenna positions at which two quasi-wavefronts are closely located, the two waveforms interfere with each other. For example, Fig. 3(a) shows two waveforms scattered at two different scattering centers at $(X, Y) = (-0.9, -0.8)$, where the horizontal and vertical axes are a range and an electric field, respectively. The dashed and solid lines are, respectively, the first and second waves $r_1(Z)$ and $r_2(Z)$. The received signal $r_1(Z) + r_2(Z)$, in a noiseless case, is shown in Fig. 3(b).

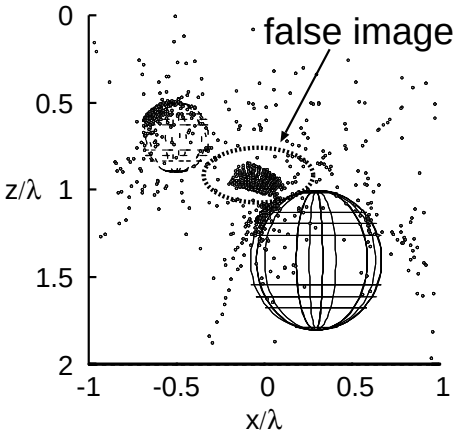


Fig. 5. Estimated target shape using the sequential subtraction method (without noise).

### 3.2 Investigation of Numerical Performance of Conventional Methods

We show the results of the sequential subtraction method applied to the signal $r_1(Z) + r_2(Z)$ in Fig. 3(b). First, the estimated first waveform $r_1(Z)'$ is subtracted from $r_1(Z) + r_2(Z)$, giving the residual waveform $r_1(Z) + r_2(Z) - r_1(Z)'$ in Fig. 3(c), which has distortion compared with the actual waveform $r_2(Z)$ in Fig. 3(a). In addition, the estimated second waveform $r_2(Z)'$ is subtracted from the residual signal $r_1(Z) + r_2(Z) - r_1(Z)'$, and we obtain the final residue in Fig. 3(d). Here, the estimated time delay of $r_2(Z)$ is incorrect because $r_1(Z) + r_2(Z) - r_1(Z)'$ in (c) is different from the actual waveform $r_2(Z)$. As a result, all the quasi-wavefronts are estimated as in Fig. 4, and we obtain the estimated image by applying the IBST to the quasi-wavefronts as in Fig. 5. In this figure, the points depict the estimated image while the true shapes are depicted with solid lines. Points surrounded by a dashed line correspond to a false image, created by incorrectly connecting quasi-wavefronts.

To enable a quantitative discussion, we introduce the RMS error of an estimation. Let the number of estimated points be $D$, and the minimum distance between the $i$-th estimation point and the true target shape be expressed as $\Delta r_i$. Then the RMS error of an estimation $\varepsilon$ is defined as

$$\varepsilon = \sqrt{\frac{1}{D}\sum_{i=1}^{D} |\Delta r_i|^2}. \tag{5}$$

The RMS error of Fig. 5 is calculated as $\varepsilon = 0.217\lambda$. In a noisy case where S/N=30dB, $\varepsilon = 0.204\lambda$ is calculated. The RMS errors are large in both cases due to the miss-connected quasi-wavefronts. The sequential subtraction method does not work well, even for a relatively simple target model such as the one discussed above.

Next, we examine the imaging performance of the fuzzy-SEABED method. Figures 6 and 7 show the estimated images using the fuzzy-SEABED method in a noiseless case and noisy case with S/N=30dB, respectively. The RMS errors of these images are $\varepsilon = 0.0213\lambda$ and $0.0846\lambda$, respectively. Compared with the sequential subtraction method, the estimation accuracy is high. However, this method is sensitive to noise, and the RMS error increases by 4 fold with an S/N of 30dB.

## 4. Proposed Imaging Method with Global Optimization

In previous works [1], [4], a locally optimum connection scheme was adopted for the quasi-wavefront extraction, making it difficult for application in interference-rich environments. In this study, we globally optimize quasi-wavefronts while considering all the data taken at multiple antenna positions, instead of the local optimization in conventional methods. In addition, the proposed method takes

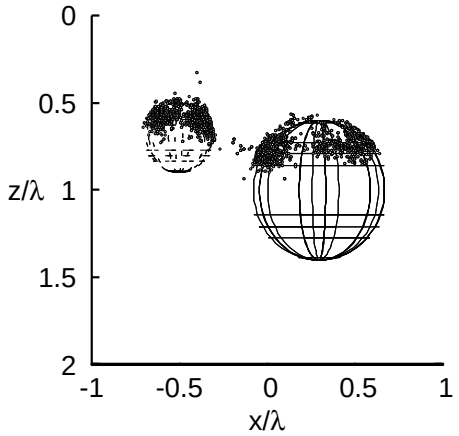


Fig. 6. Estimated image using fuzzy-SEABED method (without noise).

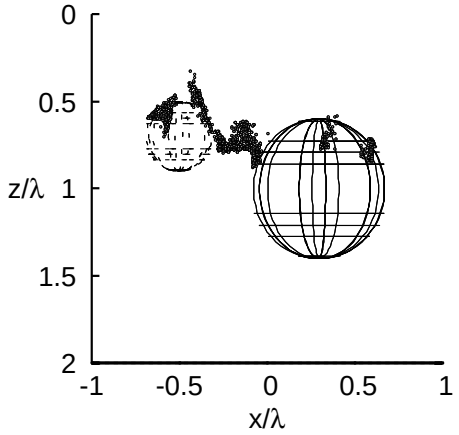


Fig. 7. Estimated image using fuzzy-SEABED method (with S/N=30dB).

into account the waveform information that is not used in conventional algorithms. The utilization of waveforms stabilizes the estimation in noisy environments.

In the proposed method, we express multiple quasi-wavefronts using a parameter matrix $V$. We can obtain the simulated signals $s_{\text{gen}}(X, Y, Z, V)$ from the calculated quasi-wavefront $q(X, Y, V)$ generated by $V$. We minimize the difference between these simulated signals $s_{\text{gen}}$ and the actual observed signals $s_0$ to determine $V$ as

$$V^* = \arg\min_V e(V), \tag{6}$$

$$e(V) = |s_0 - s_{\text{gen}}(V)|^2. \tag{7}$$

For convex target shapes, the quasi-wavefronts are always smooth [7], so the discretely sampled points of quasi-wavefronts are almost equivalent to the original quasi-wavefronts because interpolation techniques can be used for the reconstruction of the original quasi-wavefronts. The proposed method samples the quasi-wavefronts at constant intervals with $M \times M$ points in the $X$ and $Y$ directions. The assumed number of quasi-wavefronts is denoted by $W$, and the parameter matrix $V$ is expressed as

$$V = \begin{pmatrix} \boldsymbol{v}_{11} & \cdots & \boldsymbol{v}_{1M} \\ \vdots & \ddots & \vdots \\ \boldsymbol{v}_{M1} & \cdots & \boldsymbol{v}_{MM} \end{pmatrix} = (\boldsymbol{v}_{ij}), \tag{8}$$

$$\boldsymbol{v}_{ij} = (v_{ij1}, \cdots, v_{ijW}) = (v_{ijk}). \tag{9}$$

The proposed method uses the 3rd order 3-dimensional B-spline interpolation algorithm to obtain the simulated quasi-wavefronts $q(X, Y, V)$. With this interpolation, the time delay $Z$ at an antenna position $(X_i, Y_j)$ can be calculated, and is denoted by $\widetilde{\boldsymbol{v}_{ij}} = (\widetilde{v_{ijk}})$. The simulated signal $s_{\text{gen}}(\widetilde{\boldsymbol{v}_{ij}})$ at this antenna position $(X_i, Y_j)$ is expressed by the reference signal $p(Z)$ as

$$s_{\text{gen}}(\widetilde{\boldsymbol{v}_{ij}}) = \sum_{k=1}^{W} p(Z - \widetilde{v_{ijk}}). \tag{10}$$

This equation means that $s_{\text{gen}}$ is simply $p(Z)$ shifted by the time delay $\widetilde{v_{ijk}}$. This simple signal model shortens the calculation time for the entire global optimization. The local objective function $e_{\text{l}}(\widetilde{\boldsymbol{v}_{ij}})$ at antenna position $(X_i, Y_j)$ is expressed as

$$e_{\text{l}}(\widetilde{\boldsymbol{v}_{ij}}) = \int \left| s_0(X_i, Y_j, Z) - \sum_{k=1}^{W} p(Z - \widetilde{v_{ijk}}) \right|^2 \mathrm{d}Z. \tag{11}$$

The objective function $e(V)$ in Eq. (7) is expressed as the summation of Eq. (11) for $i$ and $j$

$$e(V) = \sum_{i,j=1}^{A} e(\widetilde{\boldsymbol{v}_{ij}}), \tag{12}$$

$$= \sum_{i,j=1}^{A} \int \left| s_0(X_i, Y_i, Z) - \sum_{k=1}^{W} p(Z - \widetilde{v_{ijk}}) \right|^2 \mathrm{d}Z \tag{13}$$

The procedure we used for extracting quasi-wavefronts is realized by the optimization problem to find the best $V$ that gives the minimum $e(V)$.

## 5. Application Examples of the Proposed Method

Fig. 8 shows the flow chart of the proposed imaging method including the process of extracting quasi-wavefronts. This method consists of

- initial value determination,
- global optimization, and
- final local optimization.

The dimension of the optimization problem in the global optimization step is $M^2W$. In the following numerical simulations, we assume that the number of samples is $M = 5$. We also assume that $W = 2$, which is equal to the true number of quasi-wavefronts for simplicity.. This yields a 50-dimensional optimization problem for the imaging of two targets.

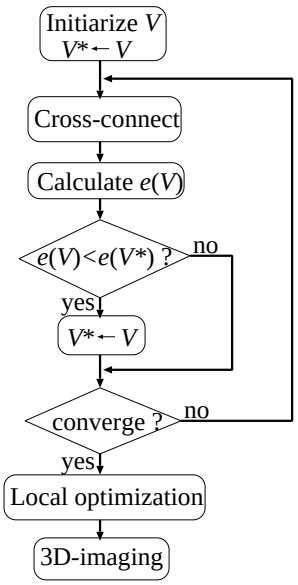


Fig. 8. Proposed extraction method for quasi-wavefronts.

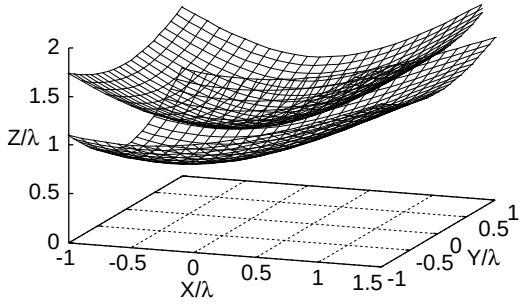


Fig. 9. Estimated quasi-wavefronts as the Initial value of the proposed method.

### 5.1 Initial Value Determination

First, every element $v_{ijk}$ of $V$ is determined by the sequential subtraction method [4], and then the optimum time delay points for each antenna position are found to minimize Eq. 11). We utilize the Levengerg-Marquardt method with a $W$ dimension for the optimization. This local optimization improves the estimation accuracy especially in the area with interferences. Next, we tentatively connect the extracted points $(X_{p_i}, Y_{p_j})$ as

$$v_{ij1} \leq v_{ij2} \leq \cdots \leq v_{ijW}, \tag{14}$$

which gives us the initial value $V_0$. Figure 9 shows a part of the estimated quasi-wavefronts as the initial value. Compared with the true quasi-wavefronts in Fig. 2, we see that the points are not correctly connected.

### 5.2 Global Optimization Process

Next, using the initial value $V_0$ determined in the previous section, we change the connections of the points by updating $V$, and recalculate the objective value $e(V)$. If the new evaluation value is better than the previous best value, parameter $V$ is adopted as the new best solution, as illustrated in Fig. 8.

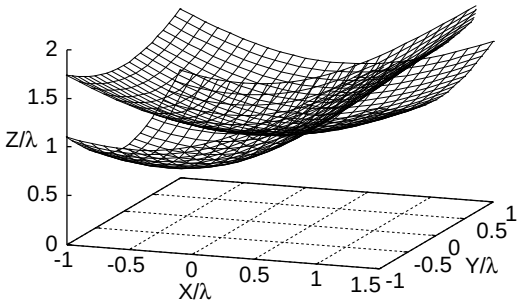


Fig. 10. Estimated quasi-wavefronts from the cross-over process.

For example, to calculate a single value of $e(V)$, which is the dominant factor in the global optimization process, requires about 150ms using an Intel Core2Duo 1.86GHz processor. Therefore, the calculation time for the global optimization process is approximately proportional to the number of iterative numbers. The number of elements in $V$ is $M^2W$, and the number of possible connection patterns is $(W!)^{M^2-1}$. For the assumed case where $M = 5$ and $W = 2$, we need to check $2^{24}$ possible patterns, which corresponds to about 700 hours of processor time. This is clearly not-practical.

To overcome the problem of excessive calculation time, we simplify the connection model. First, we randomly set a straight line on the $X$-$Y$ plain. We interchange the values of quasi-wavefronts $v_{ijk_1}$ and $v_{ijk_2}$ if $(X_i, Y_j)$ is in one of the two areas divided by the random straight line. We call this process a "cross-over" and the above-mentioned straight line a "cross-over line". The cross-over line is determined by two points on the line $(X_{i_1}, Y_{j_1})$ and $(X_{i_2}, Y_{j_2})$, which are randomly selected for each iteration.

Figure 10 shows the estimated quasi-wavefronts after the global optimization with cross-over processes. We see that the estimation accuracy is improved compared with the initial estimation in Fig. 9. Figure 11 shows the relationship between the evaluation value and iteration number using 5 different random seeds. In this figure, the evaluation value is normalized by the initial evaluation value. The required number of iterations is about 100, which is remarkably faster than an entire search with $2^{24}$ possibilities.

### 5.3 Final Local Optimization

After completing the global optimization discussed above, the best parameter $V^*$ is used as the initial value for the final local optimization described in this section. For each antenna position $(X_i, Y_j)$, a $W$-dimensional Levengerg-Marquardt method is applied to minimize the local evaluation value in Eq. (11). The average number of optimization steps is about 8, while the total time for $A^2 = 1,521$ times optimization requires about 40 seconds using the same process described above.

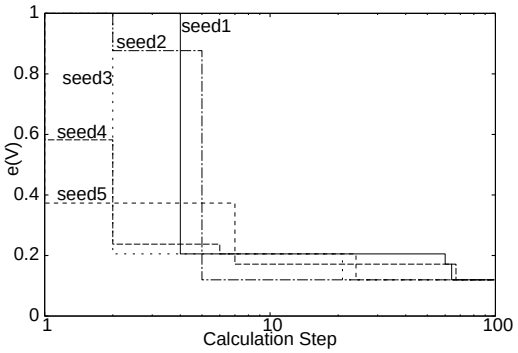


Fig. 11. Relationship between evaluation value and iteration number.

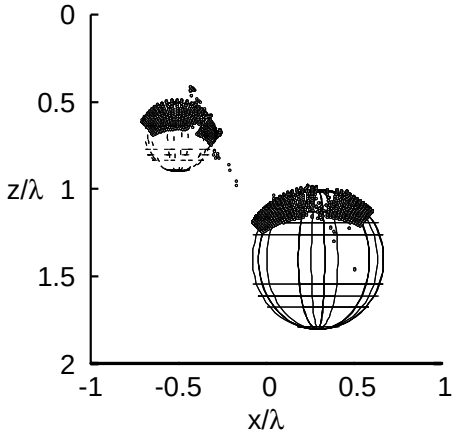


Fig. 12. Estimated image using the proposed method (without noise).

### 5.4 Accuracy Evaluation and Calculation Time

Figures 12 and 13 show the estimated images using the proposed method in noiseless and noisy, with S/N=30dB, environments, respectively. Table I shows the RMS errors of the estimated images. For the fuzzy-SEABED method, noise with S/N=30dB increases the RMS error about 4 fold, while the influence of the noise is about 1.1 for the proposed method. This proves the stability of the proposed method against noise. Moreover, the accuracy of the proposed method is 2.8 times higher for S/N=30dB compared with that of the fuzzy-SEABED method.

As for calculation time, the fuzzy-SEABED method needs 50 seconds while the proposed method needs 15 seconds for the global optimization and 40 seconds for the local optimization. Thus the fuzzy-SEABED method is lightly faster than the proposed method.

TABLE I

ESTIMATION RMS ERROR $\varepsilon$ FOR EACH IMAGING METHOD IN AN INTERFERENCE-RICH ENVIRONMENT.

| Method | without noise | S/N=30dB |
|---|---|---|
| Sequential subtraction method | $0.217\lambda$ | $0.204\lambda$ |
| Fuzzy-SEABED | $0.021\lambda$ | $0.085\lambda$ |
| Proposed method | $0.028\lambda$ | $0.031\lambda$ |

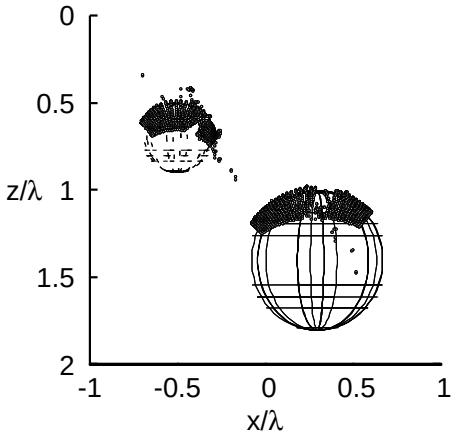


Fig. 13. Estimated image using the proposed method (S/N=30dB).

### 6. Conclusions

We have investigated the performance of conventional methods, SEABED, fuzzy-SEABED, and the sequential subtraction method for interference-rich environments. We have proposed a new method for extracting quasi-wavefronts based on global optimization. We have introduced simplified models to reduce the calculation time for the high-dimensional optimization problem. The proposed method has almost the same accuracy as that of the fuzzy-SEABED algorithm in the absence of noise while maintaining accuracy in a noisy environment with S/N=30dB.

### REFERENCES

[1] T. Sakamoto and T. Sato, "A target shape estimation algorithm for pulse radar systems based on boundary scattering transform," IEICE Transaction on Communications vol. E87-B, no. 5, pp. 1357–1365, May 2004.

[2] J.P. Fitch, Synthetic Aparture Radar, Springer-Verlag, New York, 1998.

[3] D. L. Mensa, High Resolution Radar Cross-Section Imaging, Fourth ed., Artech House, 1991.

[4] S. Hantscher *et al.* Proc. 2007 IEEE Intl. Conf. Ultra-Wideband, W04, 2007.

[5] S. Hantscher, A Reisenzahn, and C. G. Diskus, "Through-wall imaging with a 3-D UWB SAR Algorithm," IEEE Signal Processing Letters, vol. 15, pp. 269–272, Feb. 2008.

[6] S. Kidera, T. Sakamoto and T. Sato, "High-speed UWB radar imaging algorithm for complex target boundary without wavefront connections," Proc. XXIX General Assembly of the International Union of Radio Science (URSI), Aug. 2008.

[7] T. Sakamoto and T. Sato, "A phase compensation algorithm for high-resolution pulse radar systems," IEICE Trans. Communications, vol. E87–B, no. 11, pp. 3314–3321, Nov., 2004.